tions, as reasoned above. This suggests that the ratio of the amplitudes of the induced stress should be 2:1 for illumination with light of one polarization or the other in the early stages of the measurement, before centers with triplets of As-Se-As atoms lying in the x-y plane and with the Se atoms in the y direction are "frozen" in position and no longer contribute to the overall contraction of the cantilever. Such behavior, however, could not be observed reproducibly. It is obvious that centers with an orientation of the transition dipole along the z axis are not affected by any polarized light incident along the z direction.

In the present work we have shown the possibility of reversible mechanical contraction and dilatation of an amorphous solid after the absorption of polarized light. This opto-mechanical effect may form the basis of a number of mechanical applications driven by polarized light.

REFERENCES AND NOTES

1. P. Atherton, *Laser Focus World* **30**, 107 (1994).
2. A. V. Kolobov, V. Lyubin, T. Yasuda, Ka. Tanaka, *Phys. Rev. B* **55**, 23 (1997).
3. V. M. Lyubin and V. K. Tikhomirov, *J. Non-Cryst. Solids* **114**, 133 (1989).
4. V. K. Tikhomirov and S. R. Elliott, *Phys. Rev. B* **51**, 5538 (1995).
5. J. M. Lee, M. A. Paesler, D. E. Sayers, A. Fontaine, *J. Non-Cryst. Solids* **123**, 295 (1990).
6. Ke. Tanaka, K. Ishida, N. Yoshida, *Phys. Rev. B* **54**, 9190 (1996).
7. J. R. Barnes *et al.*, *Rev. Sci. Instrum.* **65**, 3793 (1994).
8. A. M. Moulin, R. J. Stephenson, M. E. Welland, *J. Vac. Sci. Technol. B*, in press.
9. P. H. Townsend, D. M. Barnett, T. A. Brunner, *J. Appl. Phys.* **62**, 4438 (1987).
10. F. J. von Pressig, *ibid.* **66**, 4262 (1989).
11. P. Krecmer and S. R. Elliott, in preparation.
12. D. S. Kliger, J. W. Lewis, C. E. Randall, *Polarized Light in Optics and Spectroscopy* (Academic Press, New York, 1990).

13. We thank M. Frumar and M. Vlcek of the University of Pardubice for providing the facilities for making the chalcogenide films. P.K. acknowledges the Wolfson Foundation for providing financial support and A.M.M. acknowledges the financial support of the EPSRC and Unilever plc.

4 June 1997; accepted 29 July 1997

Association of Mutations in a Lysosomal Protein with Classical Late-Infantile Neuronal Ceroid Lipofuscinosis

David E. Sleat, Robert J. Donnelly, Henry Lackland, Chang-Gong Liu, Istvan Sohar, Raju K. Pullarkat, Peter Lobel*

Classical late-infantile neuronal ceroid lipofuscinosis (LINCL) is a fatal neurodegenerative disease whose defective gene has remained elusive. A molecular basis for LINCL was determined with an approach applicable to other lysosomal storage diseases. When the mannose 6-phosphate modification of newly synthesized lysosomal enzymes was used as an affinity marker, a single protein was identified that is absent in LINCL. Sequence comparisons suggest that this protein is a pepstatin-insensitive lysosomal peptidase, and a corresponding enzymatic activity was deficient in LINCL autopsy specimens. Mutations in the gene encoding this protein were identified in LINCL patients but not in normal controls.

The neuronal ceroid lipofuscinoses (NCLs) are a group of related hereditary neurodegenerative disorders that occur at a frequency of between 2 and 4 in 100,000 live births (*1*, *2*). Most forms of NCL afflict children, and their early symptoms and disease progression tend to be similar. Diagnosis is frequently based on visual problems, behavioral changes, and seizures. Progression is reflected by a decline in mental abilities, increasingly severe and untreatable seizures, blindness, and loss of motor skills. There is no effective treatment for NCL, and all childhood forms are eventually fatal. Several forms of NCL are differentiated according to age of onset, pathology, and genetic linkage. These are infantile NCL (INCL, *CLN1*), classical late-infantile NCL (LINCL, *CLN2*), juvenile NCL (JNCL, *CLN3*), adult NCL (*CLN4*), two variant forms of LINCL (*CLN5* and *CLN6*), and possibly other atypical forms (*1*, *3*). The defective genes in INCL and JNCL have recently been identified by positional cloning (*4*, *5*), but the molecular basis for LINCL has remained elusive although the defect has recently been mapped to chromosome 11p15 (*3*). There are reasons, however, to suspect that the *CLN2* gene product could have a lysosomal function. First, LINCL, like other forms of NCL, is characterized by an accumulation of autofluorescent lysosome-like storage bodies in the neurons and other cells of patients. Second, several other related disorders are caused by lysosomal deficiencies, for example, palmitoyl protein thioesterase in INCL, neuraminidase in sialidosis, and β-hexosaminidase A in Tay-Sachs disease. Third, continuous infusion of lysosomal protease inhibitors into the brains of rats induces an accumulation of ceroid-lipofuscin in neurons that resembles NCL (*6*, *7*).

We have identified a protein that is deficient in LINCL by means of a biochemical approach that relies on the fact that newly synthesized soluble lysosomal enzymes contain a modified carbohydrate, mannose 6-phosphate (man-6-P). Man-6-P functions as a targeting signal in vivo as it is recognized by man-6-P receptors (MPRs), which direct the intracellular vesicular targeting of newly synthesized lysosomal enzymes from the Golgi to a prelysosomal compartment (*8*). Purified cation-independent MPR can be used as an affinity reagent for the detection of immobilized man-6-P glycoproteins in a protein immunoblot-style assay or can be coupled as an affinity chromatography reagent for the purification of man-6-P glycoproteins (*9*–*11*).

If LINCL results from the absence or deficiency of a lysosomal enzyme, then its corresponding man-6–phosphorylated form should also be absent or decreased. To test this possibility, we fractionated detergent-soluble extracts of LINCL patient and normal control brain autopsy samples by two-dimensional gel electrophoresis, transferred them to nitrocellulose, and detected man-6-P glycoproteins with an iodinated fragment of the MPR (Fig. 1). Normal brain contains ~75 distinct spots representing multiple isoforms of various man-6-P–containing glycoproteins (Fig. 1, top). LINCL brain is similar, except that one prominent spot is absent (Fig. 1, bottom). The corresponding normal spot is ~46 kD and has an isoelectric point (pI) of ~pH 6.0. Three other LINCL specimens were examined with the consistent observation that this protein was missing.

To identify this potential candidate for CLN2, we purified man-6-P–containing glycoproteins from normal brain by affinity chromatography on a column of immobilized MPR and, after fractionation by SDS–polyacrylamide gel electrophoresis (PAGE)

D. E. Sleat, H. Lackland, C.-G. Liu, I. Sohar, P. Lobel, Center for Advanced Biotechnology and Medicine, Piscataway, NJ 08854, USA and Department of Pharmacology, Robert Wood Johnson Medical School–University of Medicine and Dentistry of New Jersey, NJ 08854, USA. R. J. Donnelly, Department of Lab Medicine and Pathology, New Jersey Medical School–University of Medicine and Dentistry of New Jersey, Newark, NJ 07103, USA. R. K. Pullarkat, New York State Institute for Basic Research in Developmental Disabilities, Staten Island, NY 10314, USA.

*To whom correspondence should be addressed.

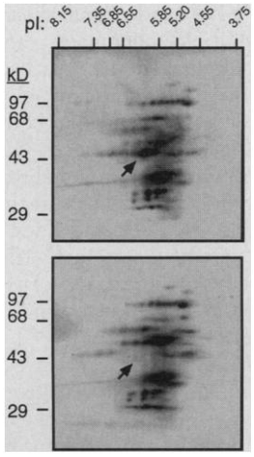

Fig. 1. A protein deficient in LINCL. Detergent-solubilized extracts of gray matter (50 μg of protein) from normal (top) or LINCL (bottom) brain autopsy specimens were fractionated by isoelectric focusing and SDS-PAGE, transferred to nitrocellulose, and man-6-P glycoproteins detected with ^{125}I-labeled MPR. The man-6-P glycoprotein that is absent in LINCL extracts is indicated with an arrow.

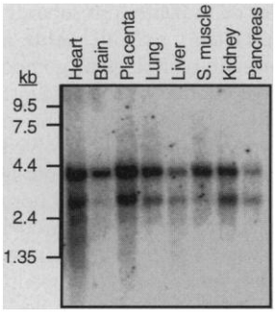

Fig. 2. CLN2 expression in various human tissues. An RNA blot of polyadenylated [poly(A)$^+$] human RNA (Clonetech, Palo Alto, California) containing 2 μg of poly(A)$^+$ RNA was probed with the ^{32}P-labeled insert of EST37588. Hybridization with two transcripts of ~2.7 and 3.7 kb is apparent in all tissues. The mRNA was also detected in spleen, thymus, prostate, testis, ovary, small intestine, colon, and peripheral blood leukocytes (*16*). The ubiquitous distribution of this mRNA as indicated by RNA blotting is confirmed by the existence of highly related clones in many different cDNA libraries as found by database searches. S. muscle, skeletal muscle.

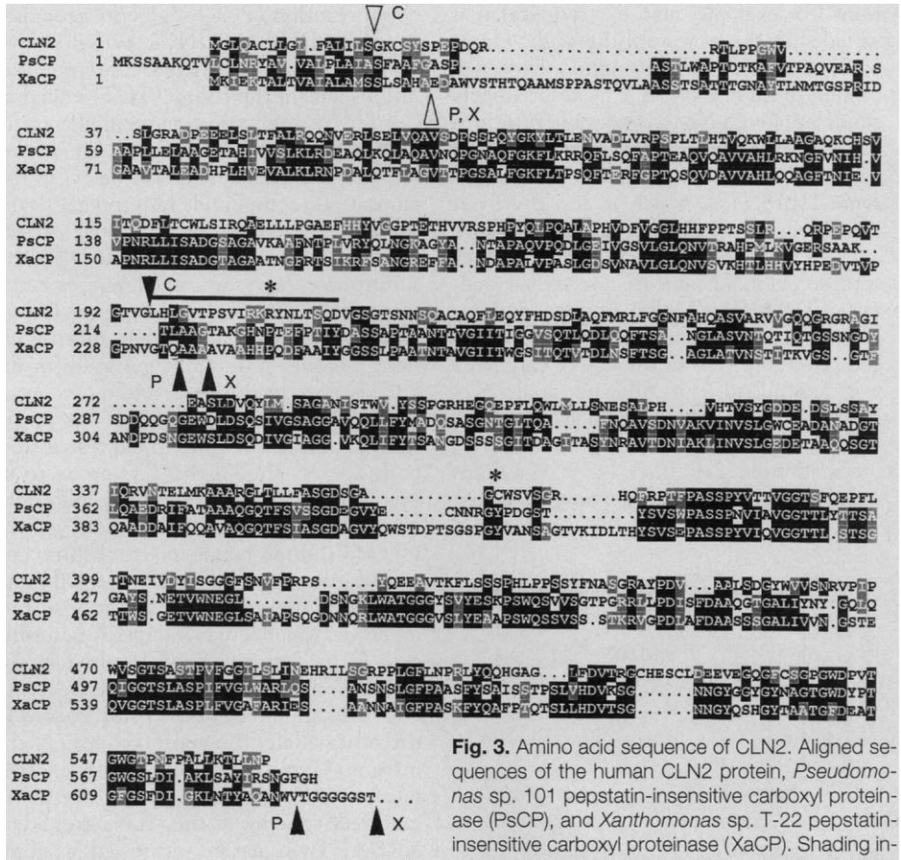

Fig. 3. Amino acid sequence of CLN2. Aligned sequences of the human CLN2 protein, *Pseudomonas* sp. 101 pepstatin-insensitive carboxyl proteinase (PsCP), and *Xanthomonas* sp. T-22 pepstatin-insensitive carboxyl proteinase (XaCP). Shading indicates regions of amino acid conservation: heavy shading indicates identical amino acids and light shading indicates similar amino acids. Predicted and known peptide cleavage sites are indicated by unfilled and filled arrows, respectively, and are labeled C, X, and P for CLN2, XaCP, and PsCP. Asterisks indicate amino acids that are mutated in LINCL patients, and the horizontal bar indicates the chemically determined peptide sequence of the 46-kD mature form heavy chain. XaCP has a 192–amino acid COOH-terminal extension that is proteolytically removed. Abbreviations for the amino acid residues are as follows: A, Ala; C, Cys; D, Asp; E, Glu; F, Phe; G, Gly; H, His; I, Ile; K, Lys; L, Leu; M, Met; N, Asn; P, Pro; Q, Gln; R, Arg; S, Ser; T, Thr; V, Val; W, Trp; and Y, Tyr.

and transfer to a polyvinylidene difluoride membrane, the band that was absent in the LINCL specimens was isolated and sequenced. The NH_2-terminal sequence was compared with predicted translation products from the expressed sequence tag (EST) database (dbEST) with the tBLASTN program. The initial search detected a murine clone encoding a sequence identical to the peptide in 16 of 20 positions, and later releases of dbEST contained human clones identical to the peptide in 19 of 20 positions. By iterative database searching and sequencing select clones, a nearly full-length sequence for the human CLN2 candidate was assembled (*12*). The 5′ end of the human cDNA was obtained from a human cortex cDNA library (*13*). This composite sequence (*14*) was confirmed from a genomic clone and genomic DNA from LINCL patients and controls.

The location of polyadenylate tracts on various human EST cDNA clones indicates that there are two transcripts, with the polyadenylate tail starting after nucleotide (nt) 2503 for the short transcript and nt 3487 for the long transcript. This was confirmed by RNA blot analysis, which revealed two transcripts of ~2700 and 3700 nt (Fig. 2). The mRNA was detected in all tissues examined with highest levels in heart and placenta and relatively similar levels in other tissues.

The CLN2 transcript long open reading frame encodes a 563-residue protein, predicted to contain a 16-residue signal sequence (Fig. 3). There are no methionines between the putative initiation codon and the start of the sequence determined by Edman degradation at residue 195, indicating that the CLN2 precursor contains a long pro-region or consists of an NH_2-terminal light and a COOH-terminal heavy chain. Because all five potential glycosylation sites reside COOH-terminal to the cleavage site, if a light chain were present in the mature protein, it would not have been detected by the man-6-P glycoprotein assay.

The predicted physical properties of the protein are in accordance with the observed properties of the protein that is missing in LINCL patients [apparent relative molecular mass (Mr) of 46,000 and pI of 6.0]. The calculated Mr of the mature protein heavy chain is 39,700. Assuming all glycosylation sites are utilized and an average Mr of 1800 for each oligosaccharide, the total Mr would be ~48,000. The calculated pI is 6.13 without considering posttranslational modifica-

tions (for example, man-6-P residues) that would shift the pI toward the acidic range.

The absence of this 46-kD lysosomal protein in LINCL patients makes it a likely candidate for CLN2. Strong support for this conclusion comes from the observation that the gene identified here maps to chromosome 11p15 (*15*), which is also the locus identified for *CLN2* by genetic linkage analysis (*3*). Direct evidence for the identification of *CLN2* came from sequence analysis of DNA from LINCL patients and unaffected family members (Table 1). The gene structure (*16*) of the *CLN2* candidate was determined, thus allowing analysis of both intronic and exonic sequences from LINCL patient DNA with genomic DNA prepared from cell lines (*17*). Mutations were observed in two of the polymerase chain reaction (PCR) segments generated from the DNA of LINCL patients. Two unrelated LINCL patients contained mutations within the codon (TGT) encoding Cys^{365}. In one case, a monoallelic transversion of T to C resulted in a Cys to Arg substitution; presumably, the defect in this patient is compound heterozygous and there is therefore an additional, as yet unidentified, mutation. Evidence that this substitution represents a deleterious mutation rather than a polymorphism is provided by the observation that another patient contains a different mutation in the same codon. In this case, a homozygous G to A transversion resulted in a Cys to Tyr substitution in the protein expressed from both alleles. Should this Cys prove to be involved in disulfide bonding, mutations are likely to be highly disruptive given the role of disulfide bonds in establishing and maintaining protein structure. Different compound heterozygous mutations were found in two affected siblings. A heterozygous C to T transversion resulted in the conversion of the codon (CGA) for Arg^{208} to an umber (TGA) stop codon. In the other allele, the conserved AG of the intronic 3′ splice junction sequence is mutated to AC, which is likely to result in incorrect splicing of the CLN2 candidate mRNA. Each parent possessed a single different mutant allele and an unaffected sibling had only the premature stop mutation in one allele, indicating conventional Mendelian inheritance of these mutations. None of these mutations was observed in the genomic clone, genomic DNA from four controls (one normal subject and three patients with unrelated diseases), or in any of the EST sequences that overlap these sites.

Sequence comparisons revealed significant similarities (*18*) between CLN2 with carboxyl peptidases from *Pseudomonas* (PsCP) (*19*) and *Xanthomonas* (XaCP) (*20*). Multiple alignments between the CLN2 protein and the two bacterial proteases revealed significant blocks of sequence similarities and that both PsCP and XaCP have long propieces, with mature NH_2termini located proximal to the known NH_2-terminus of the mature heavy-chain CLN2 (Fig. 3). PsCP and XaCP are highly unusual carboxyl proteinases that are not inhibited by pepstatin, the classical inhibitor of pepsin, cathepsin D, and other aspartyl proteases.

Normal and LINCL brain extracts contained similar pepstatin-sensitive (cathepsin D) activities (Fig. 4, right). In contrast, whereas normal brain contains an acid protease activity not inhibited by pepstatin and E-64, this activity was essentially absent from LINCL brains (Fig. 4, left). Pepstatin-insensitive carboxyl proteases have not, to date, been reported in mammals and would thus have been overlooked in earlier studies of lysosomal activities in LINCL patients. One characteristic of LINCL is the storage of mitochondrial ATP synthase subunit c in the lysosomes of patients (*21–23*), which may therefore indicate that subunit c represents a substrate for CLN2. Also, although the prominent neurological component of LINCL may be due to the susceptibility of neurons to metabolic insults, one intriguing possibility is that CLN2 is involved in processing of neuron-specific trophic factors.

Identification of *CLN2* will not only aid in the prevention of LINCL through genetic counseling but may reveal strategies and provide test systems for therapeutic intervention. These findings also demonstrate the utility of a general approach for determining the molecular bases for lysosomal disorders of unknown etiology.

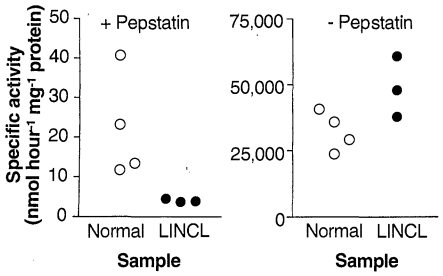

Fig. 4. Pepstatin-sensitive and -insensitive protease activities in extracts of normal and LINCL brain samples. Samples were homogenized in 50 volumes (w/v) of 0.15 M NaCl, 0.1% Triton X-100 and centrifuged at 14,000*g* for 25 min. Pepstatin-insensitive activity in the supernatant was measured with 1% bovine hemoglobin as a substrate in 25 mM formate buffer containing 2 μM pepstatin, 0.1 mM E-64, 0.15 M NaCl, and 0.1% Triton X-100 (pH 3.5). The trichloroacetic acid–soluble degradation products were quantitated with fluorescamine (*24*) in borate buffer (pH 8.6). As a control, in the absence of pepstatin, cathepsin D activity was detected in LINCL and normal extracts.

Table 1. Genotype analysis of LINCL patients.

Cell line*		Mutation†			
		Splice junction‡	C636T Arg^{208}→Stop	T1107C Cys^{365}→Arg	G1108A Cys^{365}→Tyr
C7786	Unaffected sibling	+/+	−/+	+/+	+/+
C7787	PROBAND	−/+	−/+	+/+	+/+
C7788	PROBAND	−/+	−/+	+/+	+/+
C7789	Mother	+/+	−/+	+/+	+/+
C7790	Father	−/+	+/+	+/+	+/+
WG305		+/+	+/+	+/+	−/−
WG308		+/+	+/+	−/+	+/+

*Lymphoblasts C7786 through C7790 were obtained from the human cell repository at the New York Institute for Basic Research in Developmental Disabilities and are derived from a single family with two LINCL patients; fibroblasts WG305 and WG308 are derived from two unrelated LINCL patients and were obtained from the McGill University Repository for Mutant Human Cell Strains. The parents of patient WG305 were first cousins, which likely explains the homozygosity of the observed mutation. †The symbols −/+ and −/− represent heterozygous and homozygous mutations, respectively. ‡This mutation is a G-C transversion in the genomic sequence immediately preceding T523 of the cDNA sequence.

REFERENCES AND NOTES

1. R.-M. Boustany, in *Neurodystrophies and Neurolipidoses*, vol. 66 of *Handbook of Clinical Neurology*, H. W. Moser, Ed. (Elsevier, Amsterdam, 1996), pp. 671–700.
2. J. A. Rider, G. Dawson, A. N. Siakotos, *Am. J. Med. Genet.* **42**, 519 24 (1992).
3. J. D. Sharp *et al.*, *Hum. Mol. Genet.* **6**, 591 (1997).
4. J. Vesa *et al.*, *Nature* **376**, 584 (1995).
5. The International Battens Disease Consortium, *Cell* **82**, 949 (1995).
6. G. O. Ivy, F. Schottler, J. Wenzel, M. Baudry, G. Lynch, *Science* **226**, 985 (1984).
7. G. O. Ivy, *Am. J. Med. Genet.* **42**, 555 (1992).
8. S. Kornfeld and W. S. Sly, *The Metabolic and Molecular Bases of Inherited Disease*, C. R. Sciver, A. L. Beaudet, W. S. Sly, D. Valle, Eds. (McGraw-Hill, New York, 1995), vol. 2.
9. D. E. Sleat, I. Sohar, H. Lackland, J. Majercak, P. Lobel, *J. Biol. Chem.* **271**, 19191 (1996).
10. D. E. Sleat, S. R. Kraus, I. Sohar, H. Lackland, P. Lobel, *Biochem. J.* **324**, 33 (1997).
11. K. J. Valenzano, L. M. Kallay, P. Lobel, *Anal. Biochem.* **209**, 156 (1993).
12. Human EST cDNA clones zo55e03, EST37588, and zo35g10 were sequenced in their entirety. Clones zs52e09 and zr50co6 were partially sequenced and

appear to contain cloning artifacts.
13. The 5′ end of the human cDNA was obtained by two rounds of PCR amplification of the CLN2 candidate from a human cortex cDNA library (Stratagene) by means of two different gene-specific primers and a single vector-specific primer. In the first round of PCR the T3 promoter primer was used with either gene-specific primer NR1 (5′-GTGATCACAGAATGGCACTT) or NR2 (5′-AACATGGGTTTCCGTAGGTC). In the second round of PCR, with the products from the first amplification, the T3 promoter primer and NR4 (5′-CTTCCTCAGGGTCCGCACGG) were used.
14. GenBank accession number AF017456.
15. Three lines of evidence give corroborative results for an unequivocal localization. (i) There is a nearly perfect match between nt 34 to 104 of the CLN2 cDNA candidate and GenBank accession number B04497, which represents a PCR-amplified fragment of a flow-sorted chromosome 11–specific cosmid clone. (The 317-nt B04497 also contains sequence of flanking introns.) (ii) There is a perfect 505-nt match between the 3′ end of the CLN2 cDNA (nt 2979 to 3483) and the 5′ end (nt 1 to 505) of GenBank accession number U25816. U25816 consists of 2605 nt that encompass the human TATA-binding protein associated factor II 30 ($TAF_{II}30$) gene. The $TAF_{II}30$ transcription start site is at U25816 nt 1060, and most of the promoter elements are downstream of U25816 nt 860 and thus do not overlap with the 3′ end of the large CLN2 candidate transcript. Thus, the CLN2 candidate gene and the $TAF_{II}30$ gene are physically adjacent. The $TAF_{II}30$ gene was mapped to chromosome 11p15.2-p15.5 by means of in situ hybridization [E. Scheer, M. G. Mattei, X. Jacq, P. Chambon, L. Tora, *Genomics* **29**, 269 (1995)]. (iii) Three sequences (accession numbers X72877, X72878, and X72880) representing a cosmid clone have strong matches ($P < 10^{-31}$) to nt 2817 to 3264 of the CLN2 candidate cDNA. The cosmid clone maps to chromosome 11p15. Taken together, these results indicate that the CLN2 candidate is localized to chromosome 11p15.
16. D. E. Sleat *et al.*, unpublished data.
17. *CLN2* was analyzed in patient DNA extracted from cell lines by means of overlapping M13 forward- and reverse-tailed primer pairs. Each pair amplified an exon and flanking intronic sequences, and the resulting products were sequenced with dye-labeled −21M13 primer. For patients, the sequence of fragments that mismatched with the consensus sequence was then confirmed by sequencing with the M13 reverse primer. Each fragment containing a mutation in both patients and relatives was then independently reamplified and sequenced on both strands to confirm that the observed heterogeneities were not artifacts of PCR amplification. Primer pairs that detected mutations in patient DNA were SF3 (5′-TGTAAAACGACGGCCAGTCAGACCTTCCAGTAGGGACC)/SR3 (5′-CAGGAAACAGCTATGACCCTGTATCCCACACAAGAGAT) and SF0A (5′-TGTAAAACGACGGCCAGTTAGATGCCATTGGGGACTGG)/SR0A (5′-CAGGAAACAGCTATGACCGTCATGGAAATACTGCTCCA). PCR from 1-μg samples of patient DNA with Vent DNA polymerase (New England Biolabs, Beverly, MA) was done under the following cycle conditions: 94°C for 3 min followed by 10 cycles of 94°C for 1 min, 50°C for 1 min, and 72°C for 1 min, followed by 30 cycles of 94°C for 1 min, 65°C for 1 min, and 72°C for 1 min, with a final incubation for 10 min at 72°C. Products were purified by means of Qiaquick spin columns (Quiagen, Chatsworth, CA) and cycle-sequenced with AmpliTaq DNA polymerase (Roche Molecular Systems, Alameda, CA) and ABI Prism dye-labeled primers (Perkin Elmer, Foster City, CA) on an ABI 373 automated sequencer.
18. A BLAST search of the SwissProt database with the conceptually translated CLN2 candidate gave a highly significant match with PsCP: $P = 1.9 \times 10^{-11}$; the Dayhoff comparison score is >8 SDs above the mean (ALIGN program, relative to 200 comparisons of scrambled sequences); and pairwise comparison with GCG Bestfit yields identity and similarity scores of 25 and 46%, respectively. PsCP is related (52% identical, 66% similar) to XaCP. XaCP is not detected in a BLAST search with the CLN2 candidate, but in pairwise comparisons the Dayhoff comparison score is >2.7 SDs above the mean, and the identity and similarity scores are 24 and 48%, respectively.
19. K. Oda, T. Takahashi, Y. Tokuda, Y. Shibano, S. Takahashi, *J. Biol. Chem.* **269**, 26518 (1994).
20. K. Oda *et al.*, *J. Biochem.* **120**, 564 (1996).
21. D. N. Palmer, I. M. Fearnley, S. M. Medd, *Am. J. Med. Genet.* **42**, 561 (1992).
22. D. N. Palmer *et al.*, *J. Biol. Chem.* **264**, 5736 (1989).
23. J. Ezaki, L. S. Wolfe, E. Kominami, *J. Neurochem.* **67**, 1677 (1996).
24. S. De Bernardo *et al.*, *Arch. Biochem. Biophys.* **163**, 390 (1974).
25. We thank P. S. Pullarkat for technical assistance and A. B. Rabson and S. A. Moodie for providing cDNA libraries. Supported by NIH grant DK45992 and a gift from Pfizer (P.L.) and by NIH grant NS30147 (R.K.P.).

7 July 1997; accepted 11 August 1997

Mutation of the Stargardt Disease Gene (*ABCR*) in Age-Related Macular Degeneration

Rando Allikmets,* Noah F. Shroyer,* Nanda Singh,* Johanna M. Seddon, Richard Alan Lewis, Paul S. Bernstein, Andy Peiffer, Norman A. Zabriskie, Yixin Li, Amy Hutchinson, Michael Dean,† James R. Lupski, Mark Leppert

Age-related macular degeneration (AMD) is the leading cause of severe central visual impairment among the elderly and is associated both with environmental factors such as smoking and with genetic factors. Here, 167 unrelated AMD patients were screened for alterations in *ABCR*, a gene that encodes a retinal rod photoreceptor protein and is defective in Stargardt disease, a common hereditary form of macular dystrophy. Thirteen different AMD-associated alterations, both deletions and amino acid substitutions, were found in one allele of *ABCR* in 26 patients (16%). Identification of *ABCR* alterations will permit presymptomatic testing of high-risk individuals and may lead to earlier diagnosis of AMD and to new strategies for prevention and therapy.

Age-related macular degeneration (AMD) is the most common cause of acquired visual impairment in the elderly and is estimated to affect at least 11 million individuals in the United States (*1–3*). U.S. studies show that mild forms of AMD occur in nearly 30% of those 75 years and older, and advanced forms occur in about 7% of people in this age group (*2*). Clinically, AMD is divided into two subtypes: 80% of patients have "dry" AMD, the hallmarks of which include one or more of the following: the presence of cellular debris (drusen) in or under the retinal pigment epithelium (RPE), irregularities in the pigmentation of the RPE, or geographic atrophy; 20% of patients have exudative or "wet" AMD, characterized by serous detatchment of the RPE or choroidal neovascularization or both. Severe vision loss is associated most often with geographic atrophy or exudative disease (*4*, *5*). There are no reliable therapies for dry AMD, and only about 5% of patients with the wet subtype are candidates for laser photocoagulation therapy (*4*).

AMD is a multifactorial disorder that is associated with environmental risk factors such as cigarette smoking, diet, and cholesterol level (*3*, *6*). Genetic factors also contribute to AMD (*7*, *8*), although genetic studies have been confounded by the late onset and complex etiology of the disease. One approach to identifying the genes responsible for multifactorial disorders is to study inherited diseases with similar phenotypes. Several hereditary retinal dystrophies have phenotypic similarities to AMD. Sorsby fundus dystrophy, for example, resembles wet AMD and is caused by mutations in the tissue inhibitor of metalloproteinases-3 (*TIMP3*) gene (*9*). However, no

R. Allikmets, Intramural Research Support Program, SAIC-Frederick, NCI-Frederick Cancer Research and Development Center, Frederick, MD 21702, USA.
N. F. Shroyer and Y. Li, Department of Molecular and Human Genetics, Baylor College of Medicine, Houston, TX 77030, USA.
N. Singh, A. Peiffer, M. Leppert, Department of Human Genetics, Eccles Institute of Human Genetics, University of Utah, Salt Lake City, UT 84112, USA.
J. M. Seddon, Department of Ophthalmology, Massachusetts Eye and Ear Infirmary, Harvard Medical School, Boston, MA 02114, USA.
R. A. Lewis, Departments of Molecular and Human Genetics, Ophthalmology, Pediatrics, and Medicine, Baylor College of Medicine, Houston, TX 77030, USA
P. S. Bernstein and N. A. Zabriskie, Department of Ophthalmology, Moran Eye Center, University of Utah, Salt Lake City, UT 84132, USA.
A. Hutchinson and M. Dean, Laboratory of Genomic Diversity, NCI-Frederick Cancer Research and Development Center, Building 560, Room 21-18, Frederick, MD 21702-1201, USA.
J. R. Lupski, Departments of Molecular and Human Genetics and Pediatrics, Baylor College of Medicine, Houston, TX 77030, USA.

*These authors contributed equally to this work.
†To whom correspondence should be addressed. E-mail: dean@fcrfv1.ncifcrf.gov